J Mater Sci (2010) 45:3336–3343
DOI 10.1007/s10853-010-4354-2

Organoclay/thermotropic liquid crystalline polymer nanocomposites. Part IV: organoclay of comparable size to fully extended TLCP molecules

Youhong Tang · Ping Gao · Lin Ye · Chengbi Zhao · Wei Lin

Received: 29 October 2009 / Accepted: 25 February 2010 / Published online: 11 March 2010

Abstract Organoclay with a size of 100–200 nm was successfully prepared by a combination of wet ball milling and ultrasonication methods without changing its physico-chemical properties. A nanocomposite (TC3 FS) of 3.0 wt% treated organoclay in thermotropic liquid crystalline polymer (TLCP) was prepared. The treated organoclay was of comparable size to the fully extended TLCP molecules and it formed weak interactions with them. The liquid crystallinity of the TLCP was not greatly affected by the treated organoclay at the nematic temperature of the TLCP. Rheological characterization demonstrated that the viscosity of the TC3 FS was less than one order of magnitude higher than that of the TLCP in the linear viscoelastic region, and the steady shear viscosity of the two materials was comparable in steady shear experiments. Thus, TC3 FS is a promising viscosity reduction agent for high molecular mass polyethylene (HMMPE), functioning similarly to TLCP. The 1.0 wt% TC3 FS in HMMPE has more efficient viscosity reduction ability than the 1.0 wt% TLCP in HMMPE, with lower yielding stress and yield-starting shear rate, as well as a narrower yield shear rate region. The viscosity reduction ability of the TLCP was enhanced by the treated organoclay.

Y. Tang (✉) · P. Gao
Department of Chemical and Biomolecular Engineering, The Hong Kong University of Science and Technology, Clear Water Bay, Kowloon, Hong Kong, China
e-mail: youhongtang@gmail.com

P. Gao
e-mail: kepgao@ust.hk

Present Address:
Y. Tang · L. Ye
Centre for Advanced Materials Technology, School of Aerospace, Mechanical and Mechatronic Engineering, The University of Sydney, Sydney, NSW 2006, Australia

C. Zhao · W. Lin
Centre for Advanced Marine Materials, School of Civil Engineering and Transportation, South China University of Technology, Guangzhou 510641, China

Introduction

A fundamental difference between nanofillers and conventional fillers relates to the relative sizes of the polymer molecules and the other length scales in the system. In many polymer nanocomposites (PNCs), either the filler size and/or the interfiller distances are comparable to or smaller than the size of the polymer molecules. These parametric regimes contrast with the conventional filler limit where the filler sizes and the interfiller distances are much larger than the size of the polymer molecules. Hence, extremely low loadings suffice for nanofillers to interact with each other. Polymer-mediated interfiller interactions, i.e., the filler's influence on the dynamics of polymer segments, also play a more significant role on the filler limit in nanofillers than in conventional fillers.

Pryamitsyn and Ganesan [1] have studied the mechanisms underlying the linear viscoelasticity (concentrating on the storage modulus) of PNCs. Their results suggest that many aspects of nanocomposite rheology can actually be rationalized through the additive contributions of polymer and particulate phases. Polymer–filler interactions were shown to affect the dynamics of polymer segments, thereby modulating the relaxation spectra and the contribution of polymer in the rheological aspect. It was suggested that this effect is a generalized manifestation of the "transient

networks" noted in polymers [2], except that the nanofillers act as the nodes of interacting with the polymer. Explicitly, it was shown that although the formation of a strict network requires significant filler-induced changes in the polymer segment motilities, even weaker networks can impose important effects on the linear viscoelasticity of the polymer. It is important to note that this phenomenon manifests specifically in the nanofiller regime due to the comparable dimensions of the interparticle distances and the polymers. This size compatibility allows phenomena such as polymer chain bridging to occur and to affect the rheology of PNCs. The interfacial-stress transfer at the solid–polymer interface is critical in the nanofiller regime, and it controls the magnitude of elasticity enhancement resulting from the presence of inclusions. This effect proved more relevant for PNCs, mainly due to the comparable sizes of the filler with the polymer molecules and the reduced interfiller distance [3].

Our previous work showed that with an excess of organoclays and/or organoclays of large size, the liquid crystallinity of thermotropic liquid crystallinity polymer (TLCP) was greatly affected and the nematic mesophase was lost at a temperature where the TLCP normally had a nematic mesophase [4, 5]. However, organoclays 15–25 nm in size had no effect at all on the TLCP mesophase and liquid crystallinity [6]. Also, our work demonstrated that the intercalated organoclay of various sizes caused TLCP to lose liquid crystallinity and no nematic mesophase was observed throughout the whole temperature range up to a temperature where the TLCP normally had a nematic mesophase [5]. Additionally, the embedded TLCP fiber in a polyethylene matrix displayed a regular banded structure, with the bands all perpendicular to the chain alignment direction within the TLCP filament. The chain length of the fully extended TLCP molecule, based on its number average molecular mass of 14,000 kg/kmol, was ~85 nm [7]. Images of scanning electron microscopy on the quenched extrudates show that slender TLCP filaments with widths of 40–210 nm and lengths up to 5 micrometers existed at about 30–50 nm below the surface of the extrudates [8].

In this study, we prepared a kind of organoclay by wet ball milling and ultrasonication. The organoclay had a size of 100–200 nm, which is comparable with the reported chain length of fully extended TLCP molecules [7]. 3.0 wt% of such organoclay was added in TLCP by a method combining ultrasonication, centrifugation and solution casting to form a nanocomposite (TC3 FS). The morphology, liquid crystallinity and rheological properties of the TC3 FS were characterized to elucidate the effects of the organoclay on the TLCP. The viscosity reduction abilities of TLCP and TC3 FS for high molecular mass polyethylene (HMMPE) were also analyzed.

Experimental

Materials and sample preparation

The HMMPE, Marlex HXM TR571, used in this study was kindly supplied by Philips Petroleum International Inc., USA. The melt index of TR571 is 2.5 g/10 min (ASTM D1238, 190 °C/21.6 kg). TLCP, a copolyester containing 30% *p*-hydroxybenzoic acid (*p*-HBA), 35% hydroquinone (HQ) and 35% sebacic acid (SA) in mole fraction, was synthesized and supplied by B. P. Chemicals Ltd, UK. The as-received TLCP was a light brown powder that has been characterized previously [9]. The organoclay, Closite 20A, is a natural montmorillonite modified with dimethyl dihydrogenated tallow alkyl quaternary ammonium chloride and was kindly supplied by Southern Clay Products, USA.

Initially, the as-received organoclay was treated by a wet ball milling method using a rotary ball mill (Pascall^{TM}, Pascall Engineering Co. Ltd, Crawley, UK) with ethanol as the wet medium for 18 h, and then the upper layer of the mixture was collected. The collected mixture was sonicated for 3.5 h by ultrasonic pin vibration (Branson digital sonifier 450, USA). The treated organoclay was dried and milled into a powder form before use. The nanocomposite (called TC3 FS) was prepared by a combination of ultrasonication, centrifugation and solution casting methods with the same preparation steps as the TC3 nanocomposite reported previously [4, 5].

For the HMMPE blends, the dried 1.0 wt% TC3 FS (or purified TLCP) in powder form and HMMPE in pellet form were mechanically pre-mixed at room temperature until macroscopically homogeneous. The mixture was then extruded using a Dr. Collin twin screw extruder (Dr. Collin GMBH, Germany) at 190 °C with extrusions at two different speeds (75 and 300 rad/s respectively). The extrudate was palletized and kept dry inside an oven overnight to remove any moisture formed during processing.

Experimental methods

Wide angle X-ray diffraction (WAXRD) was conducted at room temperature using a Philips powder X-ray diffraction system (Model PW 1830, The Netherlands). The TLCP and TC3 FS were characterized in film form and the organoclays were characterized in powder form. WAXRD was performed with Cu kα radiation of wavelength 1.5406 Å.

Thermal stability analysis was carried out using a Hi-Res TGA 2950 Thermogravimetry analysis (TGA) apparatus (TA instruments, USA). The organoclays were characterized in air with a heating rate of 20.0 °C/min from 50.0 to 900.0 °C.

The TC3 FS embedded in epoxy was ultra-microtomed on an ultracut microtome (Leica ultracut-R ultramicrotomed,

Germany) at room temperature to produce sections with a nominal thickness of 100 nm. The organoclays were dispersed in ethanol and droplets of solution were dropped onto carbon-coated Cu grids for observation after evaporation of the solvent. Transmission electron microscopy (TEM) images were obtained at 200 kV with a transmission electron microscope (JEOL 2010, Japan).

A Fourier transform infrared (FTIR) spectrometer (Bio-Rad FTS 6000, USA) was used at room temperature with an attenuated total reflectance mode with and without polarizer light for thin film. The film preparation method was the same as previously described [6].

The mesophase structures of the liquid-crystalline phases of the TLCP and TC3 FS were investigated by polarized optical microscopy (POM) using an Olympus microscope BX 50 with a Cambridge shear system CSS450 (Linkam Scientific Instruments Ltd., UK) connecting a hot stage at 185 °C. The detailed steps have been described previously [6].

Controlled strain rheological measurements were carried out using an advanced rheometric expansion system (ARES) (TA instruments, USA) with a 200 g cm transducer within the resolution limit of 0.02 g cm. The 50-mm parallel plate fixtures were used for all tests reported here. All measurements were performed at 185 °C in N_2 atmosphere. A controlled thermomechanical history was performed before testing [6].

The rheological behaviors of the HMMPE blends were characterized using a capillary rheometer (Göttfert Rheograph 2003A, Germany). Here, the controlled piston speed mode was used at the temperature of 190 °C with a round hole capillary die ($D = 0.7$ mm) after die radii had been calibrated; the die entrance angle was 180°. All samples had been dried in an oven at 105 °C for at least 12 h before testing.

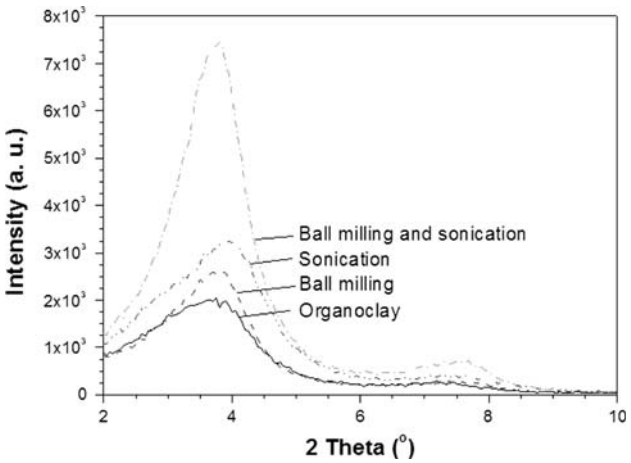

Fig. 1 WAXRD of as-received organoclay with wet ball milling and/or ultrasonication treatments

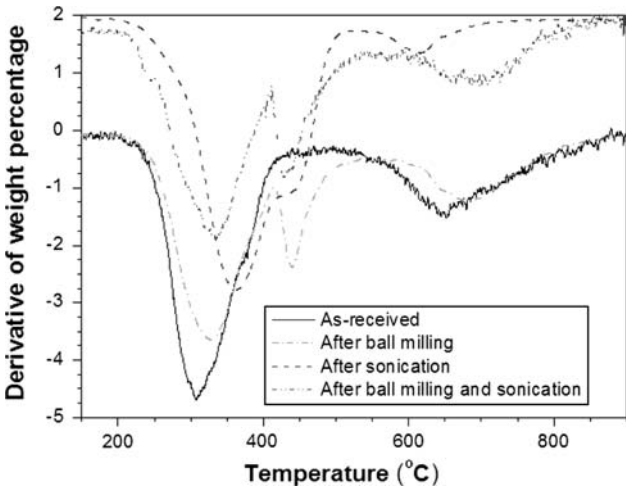

Fig. 2 DTG of as-received organoclay with wet ball milling and/or ultrasonication treatments in air condition

Results and discussion

Organoclay after wet ball milling and ultrasonication treatments

The organoclay treated by a combination of wet ball milling and ultrasonication was compared with the organoclay treated by each method individually, to elucidate the effects of such a combination on the physico-chemical properties of the organoclay. Figure 1 shows that the organoclay galley did not change with wet ball milling and/or ultrasonication, but changes in peak intensity and half height width are observed. Wet ball milling caused the peak intensity increases and ultrasonication caused the peak intensity increase further with half height width of peak also increasing slightly. The combination of the two methods broadened the half height width of the peak, as well as dramatically increased peak intensity. Those peak intensity increasing and line broadening were attributable to reduction in the size of the clay. From Fig. 1, the combination of the two methods had a more obvious effect on the organoclay size reduction.

Derivative thermogravimetry (DTG) curves are given in Fig. 2, testing the thermal stability of all kinds of organoclay in air. The curves clearly show the thermal oxidation of the organic molecules in the layered silicates, as shown in the first peak (at approximately 300–330 °C) in Fig. 2. After treatment, this peak shifts to higher temperatures with ultrasonication treatment causing more obvious shifting than other treatments. The second peak (at approximately 430–450 °C) and the third peak (at approximately 650–750 °C) resulted from the change of a substantial fraction of the surface aluminum from octahedral to tetrahedral coordination, which we associated with the

dehydroxylation of clay. In the as-received organoclay there was no second peak. After the treatment, some dehydroxylation occurred at relatively lower temperatures. That caused the second peak to appear at 430–450 °C, especially after ultrasonication treatments. Ultrasonication could also cause the third peak shift to a higher temperature, especially in the organoclay treated by the combined method.

Direct observations by TEM of the organoclay after different treatments are shown in Fig. 3: initially the as-received clay had a particle size greater than 1.0 micrometer, with a highly crystallized structure as shown in Fig. 3a and b; after wet ball milling for 18.0 h, the particle sizes of the upper layer organoclay suspension were relatively small, about 500 nm in size, but with relatively broad distribution, and the organoclay still showed highly crystalline structures in Fig. 3c and d. After ultrasonication, as shown in Fig. 3e and f, the organoclay consisted of thin plates without a regular morphology, due to both impact with other particles and shock-wave impacts on the organoclay surface. The size of the smallest particles was smaller than that observed in the ball milling clay. Figure 3g and h presents the clay morphology after the combinational method. It displays not only a reduction in particle size but also rolling of the particle edges.

With the combination of the two methods, the thermal properties and crystallization of the organoclay were not been seriously affected. By virtue of its smaller sized particles and narrower size range, as well as its adequate purification and the controllable size, the treated organoclay can be used for further studies.

Interactions between TLCP and organoclay

The absorption peak observed at 1062 cm^{-1} in the TLCP (representing asymmetric stretching of –C–O– in –Ar–C–O–Ar– of the TLCP molecule) shifted to 1055 cm^{-1} in the TC3 FS, indicating that there was interaction between the

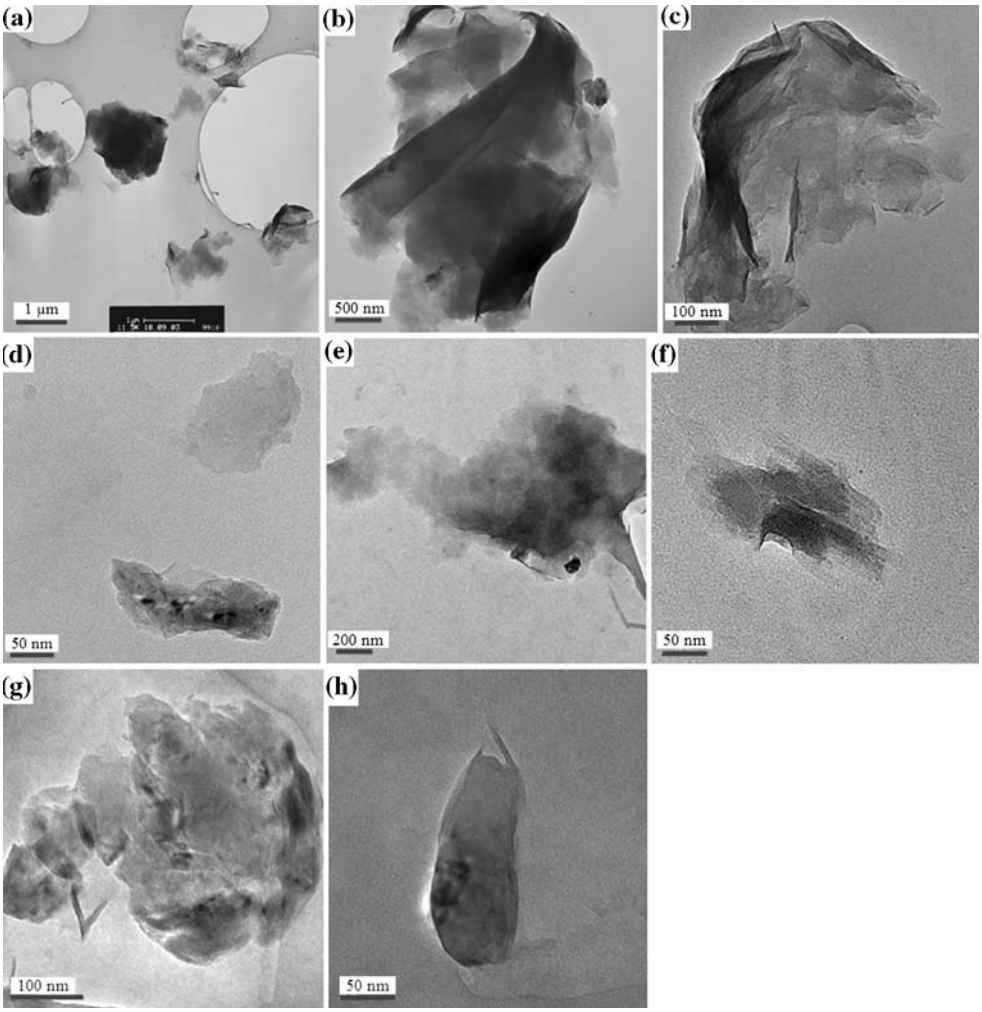

Fig. 3 TEM images of organoclays: **a**, **b** as-received; **c**, **d** after wet ball milling for 18 h; **e**, **f** after sonication for 3.5 h; **g**, **h** after wet ball milling and sonication

TLCP molecules and the layered silicate. The symmetric –C–O– stretching peak appeared at 1012 cm^{-1} in the TLCP did not shift in the TC3 FS. Also, the relative intensity ratio between the two stretching modes did not change in the TC3 FS.

Peaks at 1092 and 1180 cm^{-1} belong to the –C–O– groups in stretching mode (in –Ar–C–O–CH_2–). There was no peak shifting between the materials, but the ratio between the relative intensity of the symmetric/asymmetric stretching peaks differed. In the TLCP, the symmetric intensity was greater than the asymmetric intensity, whereas for the TC3 FS the asymmetric intensity was much greater than the symmetric intensity. Symmetric stretching was suppressed in the TC3 FS. The peaks at 1110 and 1130 cm^{-1} represent aromatic =C–H in-plane deformation vibrations. The peak at 1130 cm^{-1}, which is the dominant peak in the TLCP spectrum, was completely suppressed in the TC3 FS, as shown in Fig. 4.

The spectra obtained by FTIR spectrometry with polarized light are shown in Fig. 5. For the absorption peak at 1062 cm^{-1}, TC3 FS showed a red shift in the horizontal polarized direction and a blue shift in the vertical polarized direction. The magnitude of the red shift was larger than that of the blue one, therefore red shifting could be observed in the TC3 FS without the use of the polarizer (shown in Fig. 4). The symmetric peak of TC3 FS at 1092 cm^{-1} was suppressed in both directions. In the TLCP, symmetrical stretching in the vertical direction was suppressed. The peaks at 1110 and 1130 cm^{-1} represent C–H in-plane (ip) deformation vibrations. With vertical polarized light, the C–H ip stretching spectrum for the TC3 FS merged together and formed a peak at 1120 cm^{-1}, but in the TLCP the dominant peak occurred at 1130 cm^{-1}. With horizontal light, one type of TC3 FS C–H ip stretching peak at 1110 cm^{-1} shifted to the higher wavenumber of 1118 cm^{-1}.

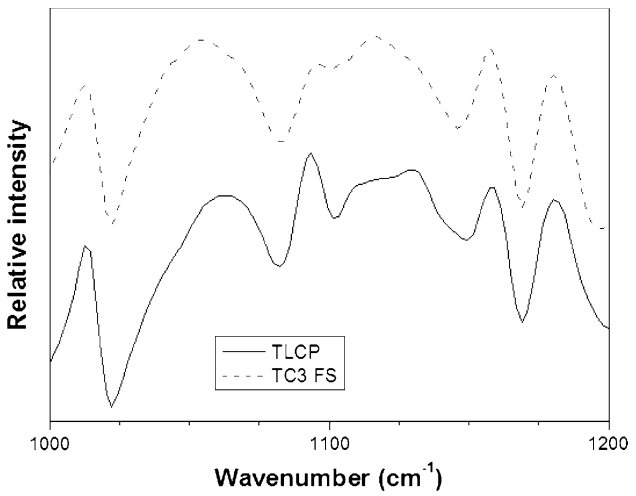

Fig. 4 FTIR of as-received TLCP and TC3 FS films at room temperature in ATR mode

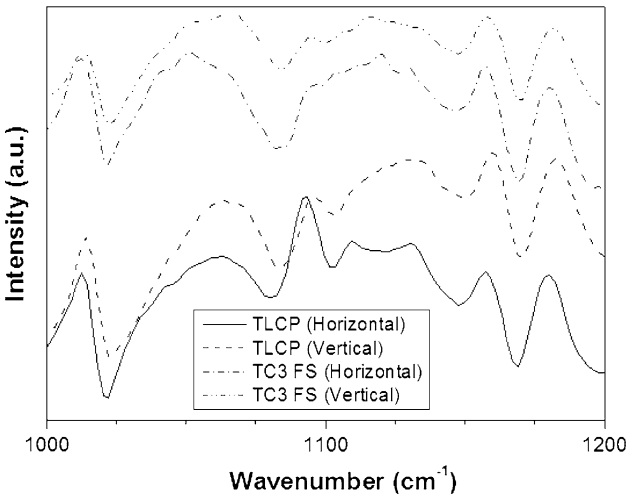

Fig. 5 Polarized FTIR of as-received TLCP and TC3 FS film using ATR mode at room temperature

From the above analysis by FTIR characterization, it is concluded that the interactions between the organoclay and TLCP exist which should affect the properties of the TLCP, especially its liquid crystallinity and rheological properties, which will be discussed in the following.

Organoclay dispersion and morphological analysis

Typical WAXRD patterns for the organoclay, TLCP and TC3 FS hybrid are shown in Fig. 6. In the WAXRD pattern, the peak for organoclay, originally at 2.35 nm, shifted to a higher value, 3.40 nm, as the gallery expanded to accommodate the intercalating polymer in TC3 FS. Second-order reflection is very common and intercalated hybrids can sometimes have up to 13 order reflections [10]. Bright-field TEM images of the treated organoclay

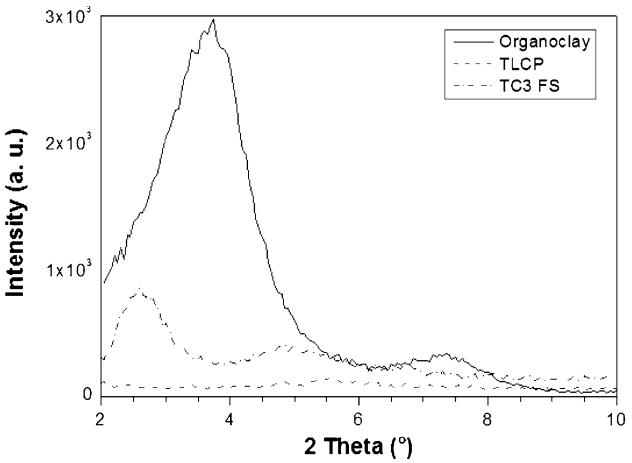

Fig. 6 WAXRD of as-received TLCP, organoclay and TC3 FS

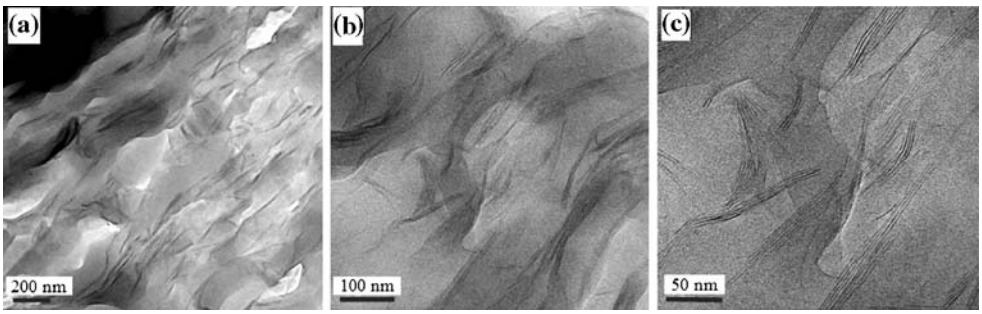

Fig. 7 TEM images of TC3 FS

intercalated with TLCP are shown in Fig. 7. Low magnification graphs (Fig. 7a and b) show organoclays dispersed in the polymer matrix at both magnification levels, with most of their agglomerations 10–20 nm in size. The peaks in the WAXRD patterns are attributed to the agglomerated layers. The periodic alternating dark and light bands represent the layers of silicate and the interlayer, respectively, with a spacing of ~3 nm between the layers. The TEM image in Fig. 7c shows that the organoclay size was uniform and within the range of 100–200 nm.

Liquid crystallinity and mesophase structure

Figure 8 presents the POM photographs of the TC3 FS in different conditions. Figure 8a shows the original TC3 FS morphology under polarized light at 175 °C. At that temperature, the TC3 FS has already melted but does not show mesophase structures. The light intensity is uniform, with only small domains. After steady shear at 185 °C for 3600 s at 0.5 1/s followed by relaxation for a sufficient time, the mesophase structures as shown in Fig. 8b and c show similarities to the TLCP. Careful examination of the whole images reveals that there are still some aggregations which are believed to be organoclay interacting strongly with TLCP molecules, but the agglomeration density is low and the domain sizes are not very large. We conclude that if the size of the organoclay is similar to that of the TLCP molecules [7], the organoclay has no marked influence on the mesophase structure formation at the nematic temperature.

Rheological properties

Figure 9 shows the dynamic strain sweep curves of TLCP and TC3 FS at 185 °C. The TC3 FS displayed less than one order of magnitude greater dynamic viscosity than the TLCP in the linear viscoelastic regions. In the linear viscoelastic region of the TLCP, G' and G'' had a similar magnitude of about 10.0 Pa·s and G'' dominates G'. In the linear regions of the TC3 FS, G' was more than two times greater than G'' and dominated the linear viscoelastic regions. With organoclay added and forming an intercalated morphology in the TLCP, the linear viscoelasticity of the TLCP changed and more solid-like behavior became evident. With regard to critical strain, the TLCP had a much greater linear viscoelastic strain, up to 20%, but the TC3 FS had only 0.5% linear viscoelastic region. The great difference between the critical strain values also proves that interactions existed in the TC3 FS and affected the rheological behavior of the TLCP. In the nonlinear regions, complex viscosity decreased dramatically in the TC3 FS. G' changed from the original 100 Pa·s to 3 Pa·s and G'' changed from 40 Pa·s to 20 Pa·s, G'' dominating G' in the nonlinear region. In the TLCP, evenstrain even went to the

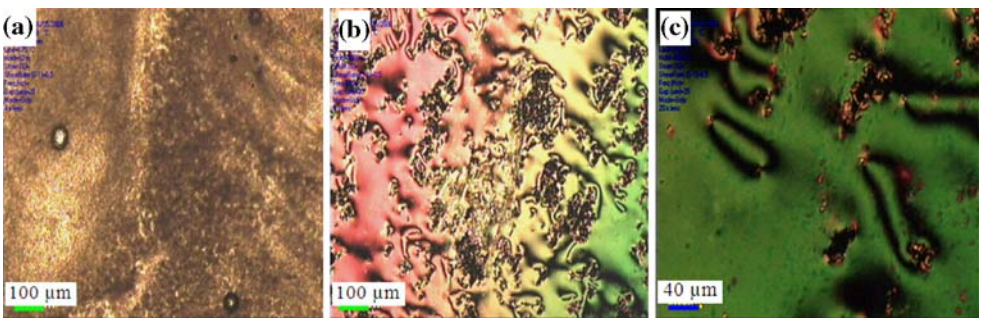

Fig. 8 POM images of TC3 FS (**a**) before steady shear at 175 °C and (**b**, **c**) after steady shear at 185 °C with shear rate 0.5 1/s for 3600 s and relaxation for more than 3600 s

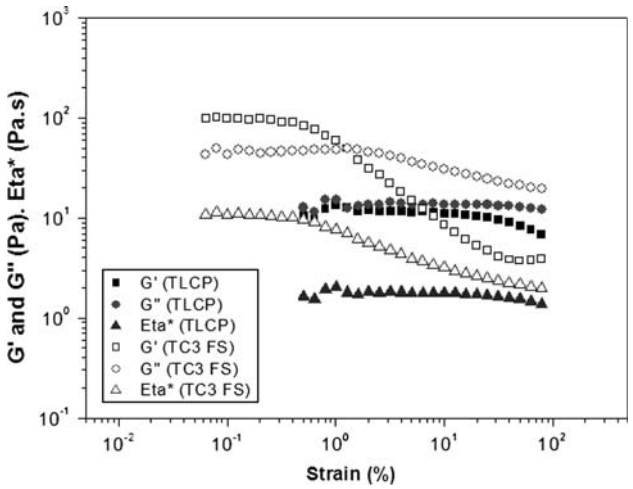

Fig. 9 Dynamic strain sweep of as-received TLCP and TC3 FS at 185 °C

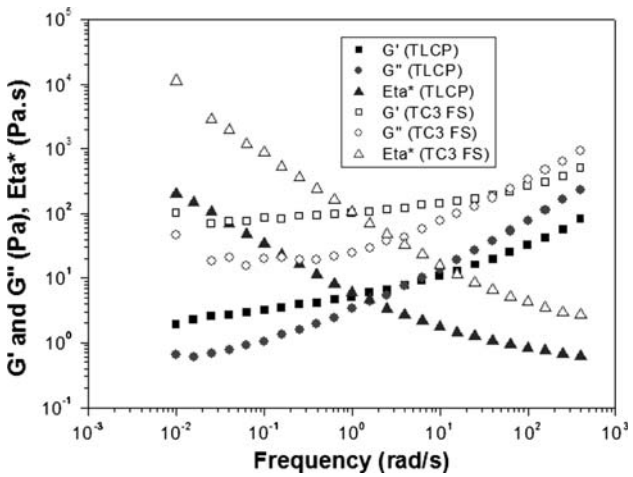

Fig. 10 Dynamic frequency sweep of as-received TLCP and TC3 FS at 185 °C

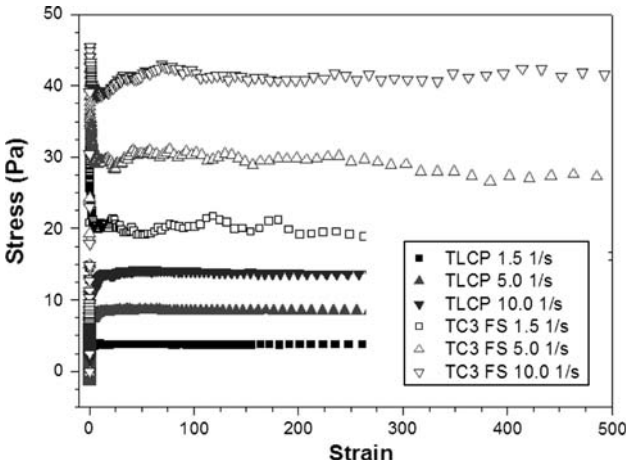

Fig. 11 Stress for as-received TLCP and TC3 FS with different shear rates at 185 °C as the function of strain

nonlinear region, G' and G'' were insensitive to strain, especially the G'' curve, and G'' still dominating G'.

Dynamic frequency sweep was performed with five decades (10^{-2} to 10^{3}) at 185 °C, as shown in Fig. 10. With careful analysis of the slopes in the low and high frequency regions, it can be clearly seen that in low frequency regions, both materials contained terminal regions, with slopes of G' and G'' being 0.207, 0.237 for the TLCP and −0.079, −0.383 for the TC3 FS. Pseudo-percolated structures existed in the TLCP molecules because of a polydomain effect [9]. With the organoclay introduced into the TLCP, the network structures were enhanced by the weak interactions (the complex viscosity of TC3 FS being just less than one order of magnitude greater than that of TLCP). Negative slopes of G' and G'' in low frequency regions were also reported by Huang and Han [11, 12] recently, who attributed this phenomenon to the influence of strong attractive interaction. In the high frequency regions, the slopes for G' and G'' were 0.634 and 0.793 for the TLCP and 0.436 and 0.740 for the TC3 FS. Neither of the slopes of G' and G'' showed flexible chain behavior, with slopes of 2 and 1, respectively. The main difference between the two is the slope of G'. At high frequencies, entanglements had already been destroyed but weak interactions still existed in both materials, with the TC3 FS maintaining stronger elastic behavior than the TLCP.

Figure 11 shows the evolution of stress at three different shear rates at a temperature of 185 °C. Molecular orientation increased monotonically, approaching a steady-state value with approximately 100 strain units for the TLCP and TC3 FS. The peak overshooting values increased but the difference between the steady state values of the TC3 FS and the TLCP at the same shear rate decreased with increasing shear rates. Figure 11 indicates the trend of maintaining a comparable steady shear viscosity at the same high shear rate.

In a series of publications, we have reported that the addition of 0.2–1 wt% TLCP to polyethylene may lead to viscosity reduction of between 88 and 95% [13, 14]. The viscosity reduction mechanism of a small quantity of TLCP in HMMPE matrix has been studied intensively [7, 15]. The chain alignment in the elongated TLCP domain caused chain alignment and disengagement in the neighboring HMMPE melt, thus the bulk viscosity of the composite drastic reduced with the PE chains changing from the random coil configuration to the extended chain configuration during elongational deformation. Figure 12 shows the apparent shear viscosity of HMMPE, 1.0 wt% TLCP/HMMPE [PT1] and 1.0 wt% TC3 FS/HMMPE [P(TC3 FS 1 wt%)] as the function of shear stress at wall at 190 °C

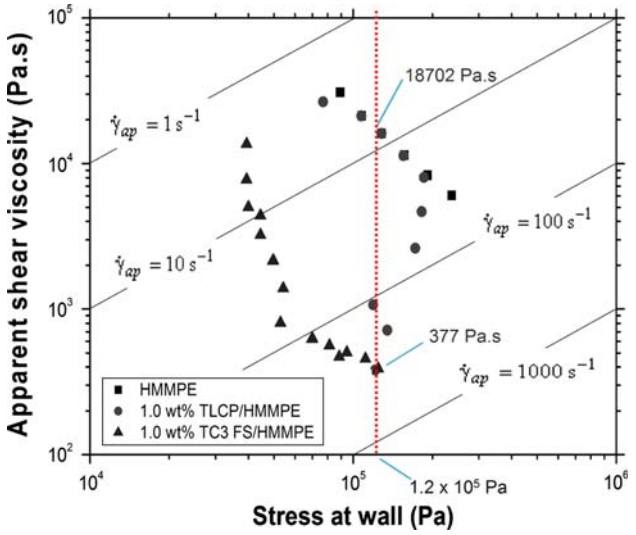

Fig. 12 Apparent shear viscosity as a function of stress at wall at 190 °C for the blends of 1.0 wt% TLCP in high molecular mass polyethylene (HMMPE) [1.0 wt% TLCP/ HMMPE] and 1.0 wt% TC3 FS in HMMPE [1.0 wt% TC3 FS/ HMMPE], measuring by capillary rheometer

with L/D = 30 and die diameter equal to 0.7 mm. From the graphs it is evident that a dramatic viscosity reduction occurred in the two blends, with a similar maximum viscosity reduction of 98% and maximum processing window up to 318.0 1/s (an equivalent wall stress of 1.2×10^5 Pa). Based on an equivalent wall stress of 10^5 Pa, the viscosity reductions for different blends were PT1 had similar viscosity to that of HMMPE, because yielding had not occurred; the viscosity of the P(TC3 FS 1.0 wt%) blend was 97.6% of that of HMMPE (corresponding apparent shear rate 188.1 1/s). The yielding stress for PT1, where the apparent shear viscosity decreased with the constant shear stress at wall [15], was 1.6×10^5 Pa; it dramatically decreased to about 0.5×10^5 Pa in the P(TC3 FS 1.0 wt%). Meanwhile, the corresponding yield start and end shear rates also modified. In the PT1 the start and end shear rates were approximately 41.0 1/s and 855.8 1/s, respectively. These decreased dramatically to 1.6 1/s and 69.7 1/s respectively in the P(TC3 FS 1.0 wt%). With the organoclay modified TLCP (TC3 FS) added into HMMPE, a much lower yielding stress and yield-starting shear rate, and a narrower yielding shear rate region occurred than in PT1. The TC3 FS had much greater viscosity reduction efficiency than the TLCP.

Conclusions

The treated organoclay with uniform size distribution of 100–200 nm, which was comparable with the size of fully extended molecules of thermotropic liquid crystalline polymer (TLCP) previously studied, was successfully prepared by wet ball milling and ultrasonication. The nanocomposite (TC3 FS) of 3.0 wt% treated organoclay in TLCP was fabricated and characterized in this study. The addition of the treated organoclay had little effect on the liquid crystallinity and mesophase structures of the TLCP. Rheological characterizations at 185 °C showed that weak interactions existed between the organoclay and TLCP, affecting the linear viscoelasticity of the TLCP. However, the viscosity of the TC3 FS was comparable to that of the TLCP, especially after steady shear. TC3 FS should be a promising viscosity reduction agent for high molecular mass polyethylene (HMMPE), functioning similarly to TLCP. Experimental results showed that with 1.0 wt% TC3 FS in HMMPE, about 98% viscosity reduction was observed and the blend had a much lower yielding stress and yield-starting shear rates, as well as a narrower yielding region than those found in 1.0 wt% TLCP in HMMPE. The viscosity reduction ability of TLCP was enhanced in the TC3 FS nanocomposite.

Acknowledgement Y. H. Tang and P. Gao gratefully acknowledge the Research Grant Council of Hong Kong (Grant number HKUST6256/02) for financial support.

References

1. Pryamitsyn V, Ganesan V (2005) Macromolecules 39:844
2. Rubinstein M, Dobrynin AV (1999) Curr Opin Colloid Interface Sci 4:83
3. Wyart FB, de Gennes PG (2000) Eur Phys J E 1:93
4. Tang YH, Gao P, Ye L, Zhao CB (2009) e-Polymer (submitted)
5. Tang YH, Gao P, Ye L, Zhao CB, Lin W (2010) J Mater Sci. doi:10.1007/s10853-010-4277-y
6. Tang YH, Gao P, Ye L, Zhao CB (2010) J Polym Sci Part B Polym Phys 48:712
7. Chan CK, Gao P (2005) Polymer 46:10890
8. Chan CK, Whitehouse C, Gao P, Chai CK (2001) Polymer 42:7847
9. Gao P, Lu XH, Chai CK (1996) Polym Eng Sci 36:2771
10. Vaia RA, Vasudevan S, Krawiec W, Scanlon LG, Giannelis EP (1995) Adv Mater 7:154
11. Huang WY, Han CD (2006) Macromolecules 39:257
12. Huang WY, Han CD (2006) Polymer 47:4400
13. Whitehouse C, Lu XL, Gao P, Chai CK (1997) Polym Eng Sci 37:1944
14. Chan CK, Whitehouse C, Gao P (1999) Polym Eng Sci 39:1353
15. Chan CK, Gao P (2005) Polymer 46:8151